

Hepatic Organic Anion Uptake in the Rat

BRUCE F. SCHARSCHMIDT, JEANNE G. WAGGONER, and PAUL D. BERK

*From the Section on Diseases of the Liver, Digestive Diseases Branch,
National Institute of Arthritis, Metabolism and Digestive Diseases, National
Institutes of Health, Bethesda, Maryland 20014*

ABSTRACT The hepatic uptake of bilirubin (BR), indocyanine green (ICG), and sulfobromophthalein (BSP) was studied in 350 anesthetized Sprague-Dawley rats by determining the initial plasma disappearance rate (V) of various doses of unlabeled ICG, or of tracer quantities of [^3H]BR or [^{35}S]BSP injected into the jugular vein simultaneously with varying amounts of unlabeled BR or BSP. Similar studies were also performed involving the simultaneous injection of potential inhibitors of hepatic uptake. The results indicate that: (a) hepatic uptake determined by direct tissue measurement could be accurately estimated from the plasma disappearance data; (b) saturation of hepatic uptake with increasing dose was readily demonstrated for each of these three organic anions, and in each instance a plot of V versus dose took the form of a rectangular hyperbola analyzable in terms of Michaelis-Menten kinetics; (c) for BR, the saturable uptake process showed a V_{max} more than 100 times the normal net transfer rate from plasma to bile; (d) hepatic uptake of BR, BSP, and ICG showed relatively selective, mutually competitive inhibition; glycocholic acid did not inhibit hepatic uptake of any of these substances; and (e) "counter-transport" could be demonstrated for each of the three test substances. These data are compatible with the existence of a carrier-mediated transport process for hepatic uptake of each of these three organic anions and clarify the relationship of hepatic BR uptake to its overall transport from plasma to bile.

INTRODUCTION

Nonvolatile metabolic waste products such as bilirubin (BR)¹, as well as many exogenously administered drugs

Part of this work was published previously in abstract form. *Gastroenterology*. 67:A-50/827; 1974.

Received for publication 1 April 1975 and in revised form 8 July 1975.

¹Abbreviations used in this paper: BR, bilirubin; ICG, indocyanine green; BSP, sulfobromophthalein; SD, Sprague

or dyes, circulate in plasma bound to albumin and are cleared from the circulation almost exclusively by the liver. For many of these substances, this transfer from sinusoidal blood to bile involves at least three steps: hepatic uptake, conjugation, and biliary excretion. Although it is possible to measure overall hepatic clearance of substances such as BR (1), it is not generally possible to quantitate each of these individual processes. While the conjugating enzyme, maximal excretory capacity, or both have been identified for some of these substances, the process of hepatic uptake and its relation to overall hepatic transport remains poorly characterized.

This paper describes studies of hepatic BR, indocyanine green (ICG), and sulfobromophthalein (BSP) uptake performed in approximately 350 intact, anesthetized Sprague-Dawley (SD) and 15 Gunn rats. Evidence is presented that suggests that hepatic uptake of each of these organic anions involves a process of facilitated transport that can be quantitated in terms of Michaelis-Menten kinetics (2), and that these anions show relatively specific, mutually competitive inhibition. In addition, the effect on hepatic uptake of physiologic variables such as fasting and the administration of enzyme inducing drugs has been studied.

METHODS

Animals. Male SD (Taconic Farms, Inc., Germantown, N. Y.) or Gunn rats (Animal Resources Branch, National Institutes of Health) weighing from 280 to 450 g were used in all studies. Before the study, each rat was anesthetized with a 50 mg/kg intraperitoneal dose of pentobarbital (Veterinary Laboratories, Inc., Lenexa, Kans.) and the right jugular vein and carotid artery were cannulated with PE-10 and PE-50 (Clay Adams, Div. of Becton, Dickinson & Co., Parsippany, N. J.) tubing, respectively. All intravenous injections were made through the jugular cannula, and arterial samples were collected into glass capillary tubes (Red Tip Micro-Natelson blood collecting tubes, Sherwood Medical Industries, Inc., St. Louis, Mo.). During these experiments, the rat's body temperature was

Dawley; UDPGT, hepatic UDP-glucuronyl transferase activity.

continuously recorded with a deep rectal probe (Tele-Thermometer, Yellow Springs Instrument Co., Yellow Springs, Ohio) and maintained at 37–37.5°C with an infra-red lamp. Unless specifically stated otherwise, rats were not fasted and only one study was performed in each animal.

Preparation of radiolabeled BR and BSP. Unconjugated [³H]BR was prepared in bile fistula dogs as previously described (3). When solutions of radiolabeled BR mixed with unlabeled BR were diazotized with para-iodoaniline according to the method of Van Roy, et al (4), an average of 96.2% of the isotope was extracted into the butyl acetate (azopigment-containing) layer. Thin layer chromatographs of butyl acetate extracts (5) with D-O silica gel (Camag Inc., New Berlin, Wis.) revealed that an average of 92% of the isotope migrated with the α_0 band (containing the dipyrrolic azopigment derived from unconjugated BR). The extinction coefficient of the [³H]BR in chloroform was 63,400 and an average of 96.1% appeared in the lower, nonpolar layer of a Weber-Schalm (6) partition. These studies indicate a high degree of radiochemical purity for this preparation of unconjugated [³H]-BR. [³⁵S]BSP was commercially prepared (Amersham/Searle Corp., Arlington Heights, Ill.). Thin layer chromatographs of this lot (SJ54) of [³⁵S]BSP run by the supplier with four different solvent systems each showed 96% or greater radiochemical purity.

Substances used for injection. BR solutions were prepared by dissolving crystalline BR (ICN Nutritional Biochemicals Div., International Chemical & Nuclear Corp., Cleveland, Ohio) in a saline-sodium carbonate solution (5.2 g each of NaCl and Na₂CO₃/liter) and then adjusting to pH 8 with 5 N HCl. The actual BR concentration in this solution was then measured in duplicate before its use for bolus injections or infusion. BR photodegradation products were formed in vitro by a method similar to that previously described (7). A concentrated (240 mg/100 ml) solution of BR in rat plasma was circulated around Westinghouse Special Blue bulbs (F20T12/BB) (Westinghouse Electric Corp., Pittsburgh, Pa.) for 16 h. Although no attempt was made to characterize these products structurally, they appeared almost exclusively in the upper layer of a Weber-Schalm (6) partition. Results from similar experiments done in this laboratory (7) also suggest that BR photodegradation products formed in this manner are about 50% bound to albumin-conjugated agarose beads (8) and poorly dialyzable. The following substances were used directly as supplied by the manufacturer: ICG, BSP (both from Hynson, Westcott & Dunning, Inc., Baltimore, Md.), ethacrynic acid (Merck Sharp & Dohme, West Point, Pa.), and sodium cephalothin (Eli Lilly and Company, Indianapolis, Ind.). Glycocholic acid was in aqueous solution at a concentration of 50 mM as prepared for injection into humans (St. Mary's Hospital Pharmacy, Rochester, Minn.) and kindly supplied by Dr. Alan F. Hofmann.

Chemical measurements. Hepatic UDP-glucuronyl transferase (UDPGT) activity was measured by the method of Black et al. (9). BR concentration in prepared solutions and in rat plasma was determined by the method of Weber and Schalm (6) or a micro-modification of this same technique. BSP concentration was measured by the method of Gaebler (10). ICG concentration in rat plasma was determined by comparing the optical density at 805 nm with standard curves of ICG dissolved in rat plasma. In studies with ICG doses of 1 mg/kg or more, plasma samples were diluted in 1% human serum albumin. In these studies

standard curves were constructed with the same dilution of rat plasma in human serum albumin and varying ICG concentrations.

Hepatic ICG content was measured by a method analogous to that of Paumgartner et al. (11). 1–3 g of liver tissue was homogenized in saline and the volume adjusted to 25 ml with saline. Total volume of the homogenate was increased to 50 ml by addition of acetone, and the mixture was shaken vigorously and centrifuged at 3,000 rpm for 15 min in the cold. The optical density at 805 nm of the supernate was read against a blank consisting of a similar extract of normal liver tissue and then compared with standard curves of ICG dissolved in a 1:1 (vol:vol) mixture of saline and acetone. With this technique, recovery of a known amount of ICG added to liver tissue homogenate averaged 101.2% in five experiments.

Radioactivity measurements. Liver tissue containing [³H]BR or [³⁵S]BSP was prepared by digestion with NCS Solubilizer (Amersham/Searle) and subsequent decolorization by addition of benzoyl peroxide in toluene and PCS solubilizer (Amersham/Searle). Radioactivity in plasma samples, aliquots of injected material, or digested and decolorized hepatic tissue was determined by liquid scintillation counting in Aquasol (New England Nuclear, Boston, Mass.). Internal standardization with [³H]toluene or ³⁵S in toluene (New England Nuclear) was used for quench correction.

Experimental protocols

Bolus injection studies. In these studies, the plasma disappearance rate of an intravenous bolus of BR, ICG, or BSP was measured. Unlabeled BR or BSP was injected simultaneously with [³H]BR or [³⁵S]BSP, respectively, and the plasma isotope disappearance rate was determined (*vide infra*). Plasma ICG concentration was determined colorimetrically as previously described. The inhibitory effect of various other substances on the plasma disappearance rate of each of these organic anions was also studied. In the inhibition experiments, unlabeled ICG or labeled plus unlabeled BR or BSP was mixed with the inhibitor in the same syringe before injection. In all studies, the total volume of injected material was kept relatively constant (0.2–0.3 ml/100 g body wt).

In studies using [³H]BR or [³⁵S]BSP, nine 100- μ l samples were obtained at 20-s intervals from 30 to 190 s after injection. ICG concentration was measured in eight samples obtained at 30-s intervals from 30 to 240 s after injection, the volume of each of these samples ranging from 100 to 300 μ l depending on the injected dose. Each capillary tube was spun at 3,600 rpm for 5 min, fractured just above the buffy coat, and the plasma was then removed for processing. The entire procedure from induction of anesthesia to collection of the final sample generally required less than 30 min.

Steady-state BR infusion studies. A second type of experiment was performed in which each rat was infused with a solution of unlabeled BR in saline-sodium carbonate buffer at rates ranging from 0.064 to 0.28 ml/kg/min. 90–120 min after the beginning of the infusion, at a time when a steady-state elevation of plasma BR concentration had been achieved, a tracer dose of [³H]BR was given intravenously and its plasma fractional disappearance rate measured with frequent arterial samples, as described above. Plasma unconjugated BR concentration was determined on at least three samples collected from as early as 1 h after the start of the infusion to immediately after the

[³H]BR injection. These values generally agreed quite closely (average deviation equaled $\pm 5.0\%$ of the mean) and their average was used in subsequent calculations. When expressed as a percentage of total BR concentration, plasma conjugated BR concentration in these studies averaged 15.8% and did not increase as BR infusion rate increased. This conjugated BR fraction has been ignored for the purposes of these calculations. Control studies were also performed, in which the rat was given an infusion (0.064–0.28 ml/kg/min) of saline-sodium carbonate buffer for 1 h before injection of the isotope. In all of these studies, the left jugular vein was used for infusion while the right jugular vein and carotid artery were used for isotope injection and sampling.

Studies of countertransport. A third type of study was performed in which each rat was given a tracer dose of [³H]BR, [³⁵S]BSP, or a 0.5 mg/kg dose of ICG, and arterial samples were collected as previously described. 2–7 min after injection, the animal was given a large intravenous bolus of unlabeled BR, BSP, or ICG and arterial sampling was continued for another 3–5 min. The purpose of these studies was to demonstrate countertransport, a phenomenon characteristic of carrier-mediated transport systems (*vide infra*).

Calculations. A semilogarithmic plot of the data points obtained during the first 2.5–4 min after injection of the test substance was generally linear (*vide infra*), and the slope, k , of this line was determined by a least squares fit to these data points. In those experiments in which BR was injected as a bolus, this plasma fractional disappearance rate, k , was used in the following equation to calculate the plasma BR disappearance rate (V_{BR})² in micromoles/per kilogram per minute.

$$V_{BR} (\mu\text{mol/kg/min}) = k (\text{min}^{-1}) \cdot D (\mu\text{mol/kg}). \quad (1)$$

In this equation D represents the injected BR dose. Plasma ICG and BSP disappearance rates were calculated similarly.

For each organic anion, several studies were done in different animals at each of several dose levels, both with and without accompanying inhibitor. The mean plasma disappearance rate (\bar{V}), as well as its SD and SE, was calculated for each dose, D . These paired values, D and \bar{V} , each determined from several studies in different rats, were used in subsequent calculations.

In Gunn rats as well as those experiments in which the rats were given an infusion of unlabeled BR followed by a tracer dose of [³H]BR, V_{BR} was calculated with the equation:

$$V_{BR} (\mu\text{mol/kg/min}) = k (\text{min}^{-1}) \cdot [\text{BR}] (\mu\text{mol/ml}) \cdot \text{PVDBR} (\text{ml/kg}) \quad (2)$$

² *Abbreviations used in these calculations and accompanying tables and figures:* C_t , plasma concentration ($\mu\text{mol/ml}$) of BR, ICG, or BSP at time t ; D , dose of organic anion ($\mu\text{mol/kg}$); Hct, peripheral venous hematocrit expressed as a fraction; I , dose of inhibitor ($\mu\text{mol/kg}$); k , plasma fractional disappearance rate (min^{-1}); $\lambda_{2,1}$, fractional hepatic uptake rate; PVDBR, plasma volume of distribution of [³H]BR (ml/kg); $q(t)$, plasma disappearance curve; t , elapsed time between injection and termination of the study; V_{BR} , plasma BR disappearance rate ($\mu\text{mol/kg/min}$); \bar{V} , mean plasma disappearance rate of BR, BSP, or ICG determined in several animals given the same dose; W_L , total liver weight (g); W_R , weight of the rat (kg).

in which [BR] is the plasma unconjugated BR concentration in the rat at the time of [³H]BR injection, and PVDBR is the plasma distribution of [³H]BR determined by extrapolating the initial data points to zero time and using the standard isotope dilution equation. The term

$$[\text{BR}] (\mu\text{mol/ml}) \cdot \text{PVDBR} (\text{ml/kg}) \quad (3)$$

by itself yields the total micromoles per kilogram of BR circulating in the plasma at the time of [³H]BR injection. Since this is equivalent to the injected BR dose (D) in micromoles per kilogram used in bolus injection studies, it is hereafter referred to as the “equivalent BR dose”. Implicit in this analysis is the assumption that BR in the extravascular (nonhepatic) compartment exchanges slowly with the plasma pool and need not be considered in these calculations. This is supported by the nearly complete hepatic recovery of injected BR (*vide infra*) as well as BR kinetic studies in man (1) and rats (12).

Data from the bolus injection studies was further analyzed in terms of Michaelis-Menten (2) kinetics. For each anion studied, values for V_{max} (representing the maximal plasma disappearance rate in micromoles per kilogram per minute) and K_m (representing the anion dose in micromoles per kilogram required to achieve the half-maximal plasma disappearance rate) were calculated by the Lineweaver-Burk (2) equation from the values for D and corresponding \bar{V} 's

$$\frac{1}{\bar{V}} = \frac{1}{D} \cdot \frac{K_m}{V_{max}} + \frac{1}{V_{max}} \quad (4)$$

by the simulation, analysis, and modeling (SAAM) program of Berman and Weiss (13).

A similar approach was used to analyze plasma disappearance data in the presence of a constant dose of inhibitor. Significant inhibition was found to be present if both of the following conditions were met: (a) the mean plasma fractional disappearance rate of a tracer dose of [³H]BR, [³⁵S]BSP, or a 0.5 mg/kg dose of ICG was significantly slower in the presence of a particular inhibitor than in its absence; (b) the value for the slope of the Lineweaver-Burk plot minus 3 SD in the presence of inhibitor was greater than the value of the slope plus 3 SD in the absence of inhibitor.

If the percent inhibition produced by a fixed dose of inhibitor decreased as the dose of the organic anion (whose plasma disappearance rate was being measured) increased, and the value for V_{max} determined by the Lineweaver-Burk plot in the presence of inhibitor was not significantly different from the value in its absence, then the data were felt to be compatible with competitive-type inhibition.

It would have also been desirable to establish that non-competitive inhibition was not present. This would require demonstration of a significant increase in the “apparent K_m ” for a particular organic anion in the presence of its inhibitor, and could best be achieved by injecting large doses of inhibitor to increase the slope maximally and decrease the absolute value of the x intercept of the Lineweaver-Burk plot without changing the y intercept. In practice, it was often impossible to use the large doses of inhibitor required without exceeding the usual volume of injection or killing the animal.

When significant inhibition was present, a value for K_I (the dose of inhibitor in micromoles per kilogram required to decrease the plasma disappearance rate of an infinitely small dose of organic anion by 50%) was calculated from

the increment in slope in the Lineweaver-Burk plot produced by the inhibitor with the following equation (2)

$$\frac{1}{\bar{V}} = \frac{1}{D} \cdot \frac{K_m}{V_{max}} \left(1 + \frac{I}{K_I} \right) + \frac{1}{V_{max}} \quad (5)$$

in which I is the dose of inhibitor in micromoles per kilogram.

Hepatic [^3H]BR, [^{35}S]BSP, and ICG content were measured as previously described and expressed as a percent of that predicted from the plasma disappearance curve with an equation of the form

$$\begin{aligned} \% \text{ predicted} \\ = \frac{\text{hepatic recovery} - (W_L \cdot C_t \cdot 0.18) \cdot (1 - \text{Hct})}{(D - D e^{-kt}) \cdot W_R} \cdot 100 \end{aligned} \quad (6)$$

In this equation, hepatic recovery is expressed in micromoles, $D - D e^{-kt}$ is the fraction of dose (in micromoles per kilogram) that has disappeared from the plasma upon termination of the study at time t , W_L is the total liver weight in grams, W_R is the weight of the rat in kilograms, C_t is the plasma concentration in micromoles per milliliter of BR, ICG, or BSP at time t , 0.18 is a correction factor (in milliliters per gram) representing the fraction of total liver weight due to contained blood (11, 14), and Hct is the peripheral venous hematocrit expressed as a fraction. The amount of BR, BSP, or ICG excreted in the bile during the first 3-4 min represents a negligible fraction ($< 1\%$)³ (11) of the injected dose and has been ignored for the purposes of these calculations.

RESULTS

Analysis of plasma disappearance curves. Fig. 1 illustrates typical plasma disappearance curves for tracer doses of [^3H]BR, [^{35}S]BSP, and a 0.5 mg/kg dose of ICG. The linear portion of both the [^3H]BR and [^{35}S]BSP disappearance curves extends to nearly 3 min, while that of the ICG curves extends to approximately 4 min. When larger doses of each of these organic anions were used (BR, over 10 $\mu\text{mol/kg}$; BSP and ICG, over 25 $\mu\text{mol/kg}$), the linear portion of the disappearance curves extended for a longer period. For consistency, the data points obtained from 30 to 170 s for [^3H]BR and [^{35}S]BSP and 30 to 240 s for ICG were used in the calculation of plasma disappearance rates.

The plasma disappearance curves of BR, BSP, and ICG, when studied over a longer time, are best represented by a sum of two or more exponential functions of the form

$$q(t) = N_1 e^{-\alpha_1 t} + N_2 e^{-\alpha_2 t} \dots N_n e^{-\alpha_n t}$$

where $q(t)$ equals the fraction of injected isotope in plasma at time t , and $N_1 + N_2 + \dots + N_n$ equals 1. The presence of n exponentials in the plasma disappearance curve of a substance implies that there are $n-1$ addi-

³ Unpublished observations.

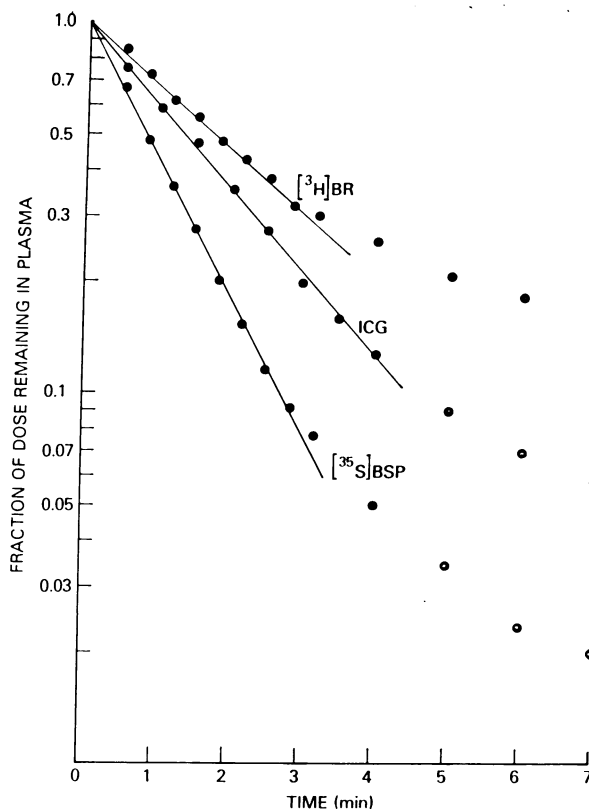


FIGURE 1 Typical plasma disappearance curves of a 0.5 mg/kg dose of ICG and tracer doses of [^3H]BR and [^{35}S]BSP injected intravenously into SD rats. Note that the linear portion of the [^3H]BR and [^{35}S]BSP disappearance curves extends to nearly 3 min, while that of the ICG disappearance curve ends at approximately 4 min.

tional pools in equilibrium with the plasma (15, 16). This system of plasma plus $n-1$ additional pools, including the intrahepatic pool, can be described in terms of a compartmental model, and such models have been formulated and validated for BR (1), BSP (17, 18), and ICG (19). For each of these models the fractional hepatic uptake rate, $\lambda_{2,1}$, is a function of all the N 's and α 's of the plasma disappearance curve, $q(t)$. However, empirically, the value of $\lambda_{2,1}$ is closely approximated by k , the initial plasma fractional disappearance rate. This has been shown to be true in normal men for both radiobilirubin ($k = 0.023 \pm [\text{SD}] 0.007 \text{ min}^{-1}$; $\lambda_{2,1} = 0.024 \pm 0.007 \text{ min}^{-1}$) and BSP ($k = 0.124 \pm 0.019 \text{ min}^{-1}$; $\lambda_{2,1} = 0.139 \pm 0.024 \text{ min}^{-1}$) (1, 20).⁴

To assess the potential magnitude of the error introduced by approximating $\lambda_{2,1}$ with k in these experiments, detailed studies of radiobilirubin kinetics were done over a period of 3 h in eight male SD rats given an average dose of 0.154 $\mu\text{mol/kg}$ of [^3H]BR, as previously

⁴ Unpublished observations.

described (12). With the SAAM program, it was found that three exponentials were both necessary and sufficient to describe the data, which were, accordingly, fitted to the three-compartmental model of BR metabolism previously postulated in human studies (1). The value calculated for $\lambda_{2,1}$ (0.310 ± 0.109) in these animals did not differ significantly ($P > 0.5$) from the initial plasma fractional disappearance rate (0.340 ± 0.073) in a group of 40 SD rats also given an average of $0.154 \mu\text{mol/kg}$ of $[^3\text{H}]\text{BR}$. Furthermore, hepatic recoveries of $[^3\text{H}]\text{BR}$, $[^{35}\text{S}]\text{BSP}$, and ICG were each measured in 12 or more rats given both low and high doses in the presence and absence of inhibitor and compared with that predicted from the plasma disappearance rate (Eq. 6). As shown in Table I, hepatic recovery of $[^3\text{H}]\text{BR}$, ICG, and $[^{35}\text{S}]\text{BSP}$ averaged 99.9%, 97.9%, and 86.8% of predicted, respectively. These results indicate that the initial plasma disappearance rate as measured in these studies agrees well with other methods of determining hepatic uptake rate; specifically, compartmental analysis and direct tissue measurement.

BR infusion studies. In 11 control studies, the plasma fractional disappearance rate of a tracer dose of $[^3\text{H}]\text{BR}$ (0.363 ± 0.052) after a 1-h infusion of saline-sodium carbonate solution did not differ significantly ($P > 0.5$) from that (0.351 ± 0.076) of 29 rats given $[^3\text{H}]\text{BR}$ without prior infusion. This suggests that the saline-sodium carbonate solution in which the BR was dissolved did not, in itself, affect hepatic BR uptake.

The results of the studies in which animals were given an infusion of unlabeled BR followed by a tracer dose of $[^3\text{H}]\text{BR}$ are presented both graphically (Fig. 2A) and in tabular form (Table II). By varying the infusion rate, a wide variety of BR concentrations ($0.6 - 53.4 \text{ mg}/100 \text{ ml}$), corresponding to a wide range of equivalent BR doses ($0.32 - 29.8 \mu\text{mol/kg}$) was produced. If saturation of hepatic BR uptake had occurred

TABLE I
Hepatic Recovery of Injected Organic Anions

Studies	Hepatic recovery	
	Mean	SE
	% predicted	
BR	99.9	5.6
ICG	97.9	5.0
BSP	86.8	5.9

Hepatic recovery of $[^3\text{H}]\text{BR}$, $[^{35}\text{S}]\text{BSP}$, and ICG has been corrected for isotope in liver plasma and expressed as a percentage of that predicted from the dose and plasma disappearance curve in each animal. These results include studies in which both low and high doses of BR, ICG, and BSP were administered both in the presence and absence of inhibitor.

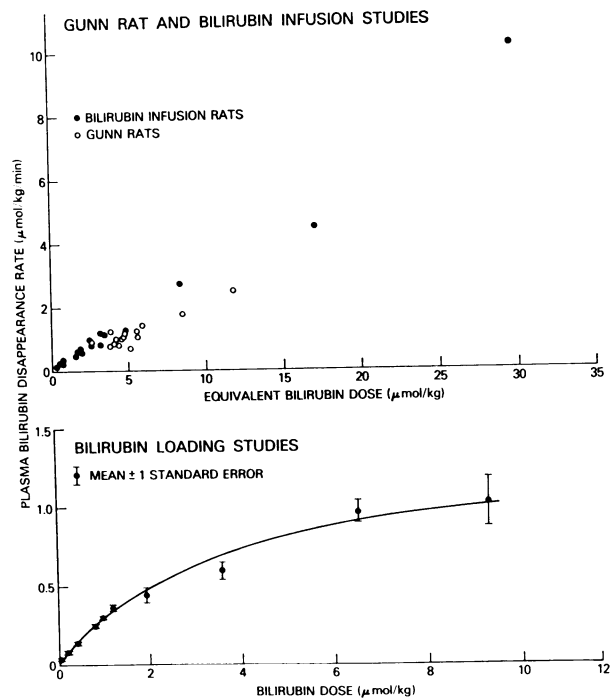


FIGURE 2 (A) V_{BR} versus equivalent BR dose for both Gunn rats and BR infusion rats. Equivalent BR dose ($\text{PVDBR} \cdot [\text{BR}]$), which represents the total quantity of BR in the plasma pool at the time of $[^3\text{H}]\text{BR}$ injection and is thus equivalent to BR dose in the loading studies, has been plotted on the abscissa rather than BR concentration to facilitate comparison with the results of BR loading studies shown in Fig. 2B. Each data point in Fig. 2A is the result of a study in one animal, while each data point in Fig. 2B is the mean ± 1 SE of values obtained from several animals. Note that while saturation of hepatic BR uptake is readily demonstrated in the loading studies, no saturation is apparent in infusion studies at even very high equivalent BR doses.

in these studies, k would be expected to decrease in an inverse hyperbolic fashion as equivalent BR dose increased. Instead, k remained relatively constant and showed no significant correlation with either BR concentration ($r = 0.126$) or equivalent BR dose ($r = 0.159$). In addition, k in this group of infused rats as a whole (0.328 ± 0.047) did not differ significantly ($P > 0.1$) from that in controls. Thus, saturation of hepatic BR uptake did not occur even at very high BR concentrations, and the plot of V_{BR} versus equivalent BR dose (Fig. 2A) is linear ($r = 0.99$; $P < 0.01$).

Gunn rat studies. The results of 15 studies in Gunn rats are also presented in Table II and Fig. 2A. The plasma fractional disappearance rate, k , of a tracer dose of $[^3\text{H}]\text{BR}$ (0.230 ± 0.055) in all Gunn rats as a group was significantly slower ($P < 0.001$) than in SD rats. However, Gunn rats appeared similar to SD rats, in that k remained relatively constant and did not correlate

TABLE II
Hepatic BR Uptake in BR Infusion Rats and Gunn Rats

BR infusion rats				Gunn rats			
[BR]	PVDBR	<i>k</i>	<i>V</i> _{BR}	[BR]	PVDBR	<i>k</i>	<i>V</i> _{BR}
mg/100 ml	ml/100 g	min ⁻¹	μmol/kg/min	mg/100 ml	ml/100 g	min ⁻¹	μmol/kg/min
0.6	3.14	0.323	0.10	5.5	4.05	0.199	0.76
0.8	4.03	0.418	0.23	5.6	2.74	0.334	0.87
1.3	2.96	0.325	0.21	5.6	4.72	0.221	1.00
1.5	2.84	0.352	0.26	6.0	3.73	0.322	1.23
3.0	3.33	0.362	0.62	6.6	3.81	0.181	0.78
3.5	2.64	0.285	0.45	6.8	3.58	0.232	0.97
3.8	2.83	0.376	0.69	6.8	4.05	0.249	1.18
4.1	2.80	0.290	0.57	7.0	4.29	0.134	0.69
4.4	4.20	0.259	0.82	7.1	4.59	0.224	1.25
4.4	3.48	0.307	0.80	7.1	4.60	0.185	1.03
4.5	3.26	0.377	0.94	7.4	3.17	0.213	0.85
6.2	3.26	0.337	1.16	7.6	3.65	0.244	1.16
6.8	2.74	0.380	1.21	8.6	4.01	0.240	1.42
7.3	3.87	0.259	1.25	12.0	4.16	0.202	1.72
18.3	2.68	0.324	2.72	16.2	4.23	0.210	2.46
28.3	3.54	0.251	4.30				
53.4	3.26	0.347	10.33				

17 SD rats were infused with unlabeled BR until a stable plasma BR concentration was achieved and were then given an intravenous dose of [³H]BR (left column). Tracer doses of radiolabeled BR were also given to 15 Gunn rats without prior infusion (right column). *k* is fractional [³H]BR disappearance rate.

significantly with either BR concentration ($r = 0.256$) or equivalent BR dose ($r = 0.332$). As with BR infusion rats, the plot of V_{BR} versus equivalent BR dose was linear ($r = 0.91$; $P < 0.01$).

Bolus injection studies. The results of studies in which SD rats were given a bolus injection of [³H]BR plus varying amounts of unlabeled BR are presented in Table III. Unlike the BR infusion studies, hepatic BR uptake showed clear-cut saturation at increasing doses, as illustrated in Fig. 2B. Lineweaver-Burk transformation of these data (Table IV, Fig. 3) allowed calculation of V_{max} (1.44 ± 0.013 μmol/kg/min) and K_m (3.93 ± 0.42 μmol/kg) as previously described. Thus, on the average, an intravenous injection of 3.93 μmol of BR, a dose sufficient to raise the plasma BR concentration acutely to about 6.2 mg/100 ml, if the average PVDBR is 37 ml/kg (12), will half-saturate hepatic uptake capacity. This is in striking contrast to the results of BR infusion studies just described in which no saturation of hepatic uptake was apparent at much higher BR concentrations.

Circulation of BR in rat plasma around Westinghouse Blue bulbs for 16 h resulted in a mixture of photodegradation products (73%) and undegraded BR (27%). This mixture was injected simultaneously with a tracer dose of [³H]BR into four rats, each receiving 1.93 μmol/kg of BR and photodegradation products formed

from 5.23 μmol/kg of BR. The plasma [³H]BR fractional rate (0.262 ± 0.022) in these animals did not differ significantly ($P > 0.2$) from that (0.226 ± 0.047) in four rats given 1.95 μmol/kg of BR alone. These results suggest that BR photodegradation products formed in this manner and given in this dose do not affect hepatic BR uptake.

The effects of ICG (40 μmol/kg), BSP (10 μmol/kg), and glycocholic acid (50 μmol/kg), on hepatic BR uptake are presented in Table III. Although glycocholic acid ($P > 0.4$) did not significantly affect the disappearance rate of a tracer dose of [³H]BR, both ICG ($P < 0.01$) and BSP ($P < 0.01$) did. Further studies in which these same doses of ICG and BSP were injected with varying amounts of BR suggested (Table IV, Fig. 3) that both ICG and BSP behave as competitive inhibitors of hepatic BR uptake. That is, they increased the slope of the Lineweaver-Burk plot without significantly altering V_{max} . Finally, it is apparent that ICG ($K_I = 206 \pm 46$) is a much weaker inhibitor of hepatic BR uptake than is BSP ($K_I = 27 \pm 2$).

The results of similar studies with ICG (Table V, Fig. 4) and BSP (Table VI, Fig. 5) were entirely analogous. Again, hepatic uptake of both of these anions showed saturation with increasing dose. For ICG, V_{max} (3.38 ± 0.17) and K_m (5.63 ± 0.53) were both somewhat larger than the corresponding values for BR and agree

TABLE III
BR Loading Studies

BR dose	Studies	Inhibitor	Inhibitor dose	k	±SD
$\mu\text{mol/kg}$			$\mu\text{mol/kg}$	min^{-1}	
0.075	29	—	—	0.351	0.076
0.219	4	—	—	0.356	0.017
0.441	7	—	—	0.303	0.056
0.824	4	—	—	0.298	0.008
1.02	3	—	—	0.296	0.010
1.27	4	—	—	0.287	0.032
1.95	4	—	—	0.226	0.047
3.61	7	—	—	0.164	0.039
6.54	4	—	—	0.148	0.022
9.29	3	—	—	0.110	0.029
0.056	3	BSP	10	0.263	0.011
0.145	3	BSP	10	0.252	0.033
0.240	3	BSP	10	0.246	0.034
0.413	3	BSP	10	0.254	0.051
0.805	3	BSP	10	0.244	0.011
1.14	3	BSP	10	0.234	0.021
2.78	3	BSP	10	0.176	0.028
6.12	3	BSP	10	0.130	0.025
0.067	5	ICG	40	0.301	0.026
0.213	3	ICG	40	0.293	0.009
8.50	3	ICG	40	0.103	0.018
0.040	7	Glycocholate	50	0.357	0.044
0.048	9	Fasting		0.350	0.033
1.44	7	Fasting		0.271	0.041
0.047	11	Phenobarbital		0.437	0.045
0.369	3	Phenobarbital		0.427	0.012
0.599	3	Phenobarbital		0.410	0.054
1.50	3	Phenobarbital		0.281	0.072
2.48	3	Phenobarbital		0.230	0.034
6.60	3	Phenobarbital		0.191	0.033
7.83	3	Phenobarbital		0.153	0.022

This table summarizes the data from BR loading studies in which the plasma fractional disappearance rate (k) of a tracer dose of [^3H]BR, injected with varying amounts of unlabeled BR, was measured with and without accompanying inhibitor, after phenobarbital pretreatment, and after fasting.

well with those obtained by previous investigators [Paumgartner et al. (11): $V_{max} = 3.74$, $K_m = 5.03$]. Hepatic ICG uptake was competitively inhibited by both BR ($K_I = 16.5 \pm 2$) and BSP ($K_I = 14.3 \pm 1.4$) with about equal efficacy, but was unaffected by glycocholic acid ($50 \mu\text{mol/kg}$). Both V_{max} (43.2 ± 4) and K_m (45.9 ± 4.4) for BSP were much larger than for either BR or ICG. Previous work by others has shown that 30% or more of intravenously injected BSP may be localized to extrahepatic tissues (21-23). This observation could explain artificially large values for V_{max} and K_m based on plasma disappearance data, particularly if the proportion of dose distributed to extrahepatic tissues increased as dose increased. However, the observed hepatic recovery of [^{35}S]BSP (Table I) suggests that extrahepatic distribution of the BSP was not a major source of artifact in these studies. In addition, distribution of even 50% of BSP to extrahepatic tissue would not, in itself, readily explain these very high values for

V_{max} and K_m , many times greater than those for BR and ICG.

Glycocholic acid ($50 \mu\text{mol/kg}$; $P > 0.2$), sodium cephalothin ($47.8 \mu\text{mol/kg}$; 20 mg/kg ; $P > 0.9$), and ethacrinic acid in a low dose ($12.3 \mu\text{mol/kg}$; 4 mg/kg ; $P > 0.4$) did not significantly alter the plasma fractional disappearance rate of a tracer dose of [^{35}S]BSP. Larger doses of ethacrinic acid ($30.7 \mu\text{mol/kg}$; 10 mg/kg), sufficient to cause overt hemolysis in some studies, did decrease k by approximately 26% ($P < 0.001$). Both ICG ($14.6 \mu\text{mol/kg}$; $P < 0.001$) and BR ($14.6 \mu\text{mol/kg}$; $P < 0.001$) did significantly and competitively inhibit BSP disappearance. ICG ($K_I = 9.2 \pm 0.6$) was a much more effective inhibitor than was BR ($K_I = 48 \pm 2$).

To test the possibility that mixing these various different substances in the same syringe before injection might have resulted in some type of chemical interaction that could introduce artifact, a smaller number of studies was done in which the inhibitor and organic anion were injected in rapid sequence (less than 10 s apart) from separate syringes. Plasma disappearance rates calculated from these studies averaged 101% of those determined from studies in which these substances were mixed before injection.

Effect of phenobarbital on hepatic BR uptake. A total of 29 rats were pretreated with 70 mg/kg/day of phenobarbital for 1 wk. Of this group, 11 rats were given a tracer dose of [^3H]BR only and the [^3H]BR

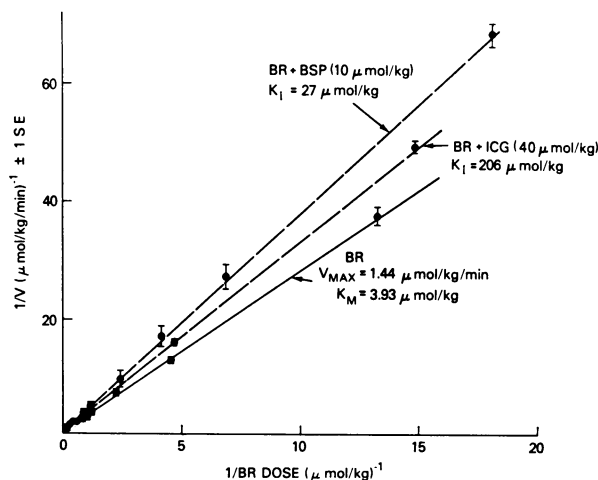


FIGURE 3 Lineweaver-Burk plots of plasma BR disappearance rates in the absence of inhibitor and in the presence of BSP and ICG. Each data point is the mean ± 1 SE of values obtained from several animals. Competitive inhibition is manifest here graphically as an increase in slope without a change in the y intercept. Note that BSP is a much more effective inhibitor of plasma BR disappearance than is ICG.

TABLE IV
Hepatic Uptake of BR, ICG, and BSP in Normal, Fasted, and Phenobarbital-Pretreated_Rats

Organic anion	Inhibitor	Inhibitor dose	V_{max}	SD	K_m	SD	Slope*	SD	K_I	SD
		$\mu\text{mol/kg}$	$\mu\text{mol/kg/min}$		$\mu\text{mol/kg}$				$\mu\text{mol/kg}$	
BR	—	—	1.44	0.13	3.93	0.42	2.726	0.068	—	—
BR	BSP	10	1.71	0.18	6.38†	0.72	3.738†	0.057	27	2
BR	ICG	40	1.37	0.35	4.45	1.23	3.255†	0.115	206	46
BR	Phenobarbital	—	1.67	0.23	3.58	0.56	2.145†	0.067	—	—
BR	Fasting	—	1.67	1.25	4.73	3.84	2.830	0.283	—	—
ICG	—	—	3.38	0.17	5.63	0.53	1.664	0.101	—	—
ICG	BR	10	3.61	0.17	9.64†	0.72	2.671†	0.114	16.5	2
ICG	BSP	12	3.63	0.85	11.11†	2.87	3.063†	0.159	14.3	1.4
ICG	Fasting	—	2.06	0.84	4.26	2.02	2.068†	0.167	—	—
BSP	—	—	43.2	4.0	45.9	4.4	1.063	0.012	—	—
BSP	ICG	14.6	32.1	10.2	88.2	33.5	2.751†	0.294	9.2	0.6
BSP	BR	14.6	34.1	6.5	47.3	3.2	1.387†	0.010	48	2
BSP	Fasting	—	18.0	16.5	23.7	22.0	1.313†	0.040	—	—

V_{max} , apparent K_m , and (where applicable) the inhibitor constant, K_I , are summarized for studies in which varying doses of BR, ICG, or BSP were injected either alone or simultaneously with a fixed dose of inhibitor.

* Slope of Lineweaver-Burk plot in minutes.

† Values significantly different from controls ($P < 0.05$).

plasma fractional disappearance rate was compared with that in 29 controls. 18 were given [^3H]BR tracer plus varying amounts of unlabeled BR. Liver weight was measured in 25 animals, hepatic UDPGT activity was measured in 19 animals, and these values were compared with liver weight and hepatic UDPGT activity in 45 and 16 control SD rats, matched for body weight, respectively. Four Gunn rats were also given tracer doses of [^3H]BR before and after identical phenobarbital pretreatment, each rat serving as his own control. After the second study, hepatic UDPGT activity and liver weights were measured and the latter compared with six untreated Gunn rats matched for body weight.

The results of these studies are summarized in Table VII. In SD rats, phenobarbital pretreatment resulted in a 24.4% increase ($P < 0.001$) in liver weight (expressed as a percent of body weight), a 70% increase ($P < 0.001$) in UDPGT activity (expressed per gram liver), and a 24.3% increase ($P < 0.01$) in k for a tracer dose of [^3H]BR. Gunn rats, which had no measurable UDPGT activity, showed a 28.2% increase ($P < 0.01$) in liver weight and a 26.7% increase ($P < 0.05$) in k for a tracer dose of [^3H]BR. These results suggest that the accelerated hepatic BR uptake produced by phenobarbital closely parallels the increase in liver weight and is unrelated to simultaneous changes in UDPGT activity.

The plasma fractional disappearance rates in phenobarbital-pretreated SD rats given varying doses of unlabeled BR in addition to the [^3H]BR tracer are listed

in Table III. The value (Table IV) for V_{max} (1.67 ± 0.23) calculated from these studies was somewhat larger than in controls and that for K_m (3.58 ± 0.56) was somewhat lower. However, these differences were not statistically significant ($P > 0.3$ for both).

Effect of fasting on organic anion uptake. The plasma disappearance rate of both a low dose and high dose of BR, ICG, and BSP was measured in a total of

TABLE V
ICG Loading Studies

ICG dose	Studies	Inhibitor	Inhibitor dose	k	\pm SD
$\mu\text{mol/kg}$			$\mu\text{mol/kg}$	min^{-1}	
0.645	5	—	—	0.522	0.033
1.290	3	—	—	0.441	0.057
6.45	3	—	—	0.306	0.014
32.3	3	—	—	0.084	0.004
64.5	3	—	—	0.056	0.008
0.645	3	BSP	12.2	0.310	0.014
1.290	3	BSP	12.2	0.276	0.039
32.3	3	BSP	12.2	0.085	0.014
0.645	3	BR	10.0	0.351	0.014
1.290	3	BR	10.0	0.336	0.045
32.3	3	BR	10.0	0.086	0.003
1.290	4	Glycocholate	50	0.423	0.059
0.645	5	Fasting	—	0.420	0.013
6.45	5	Fasting	—	0.192	0.042

Data from ICG-loading studies in which the plasma fractional disappearance rate (k) of varying doses of intravenously injected ICG was measured with and without accompanying inhibitor and after fasting.

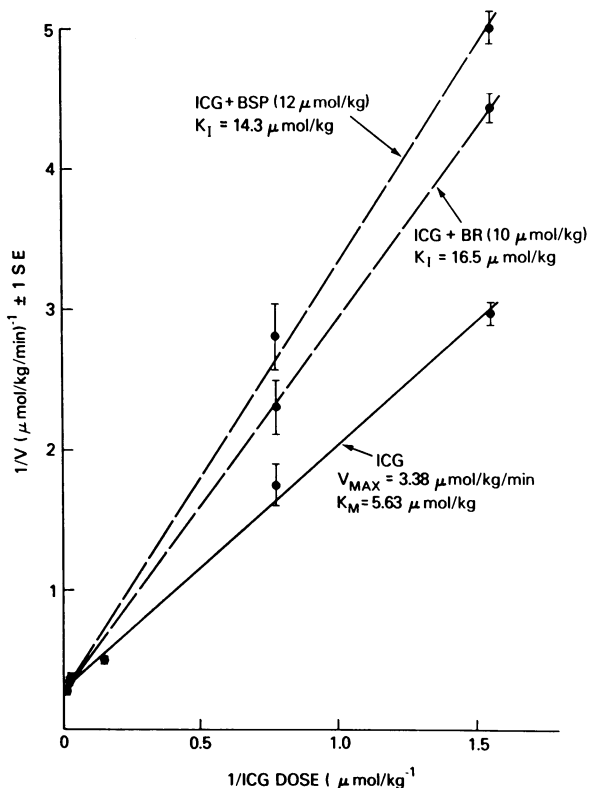


FIGURE 4 Lineweaver-Burk plots of plasma ICG disappearance rates in the absence of inhibitor and in the presence of BSP and BR. Each data point is the mean \pm 1 SE of values obtained from several animals. Note that BSP and BR both competitively inhibit plasma ICG disappearance with about equal efficacy.

44 rats allowed access only to water for 72 h before the study. This period of fasting caused an average 9.7% decrease in body weight, and a 28.8% ($P < 0.001$) decrease in liver weight expressed as a percent of body weight. As shown in Table III, fasting did not significantly affect the plasma BR disappearance rate of either dose, and values for V_{max} (1.67 ± 1.25) and K_m (4.73 ± 3.84) (Table IV) are similar to controls.

In contrast, the plasma ICG fractional disappearance rate (Table V) was decreased by 19.5% ($P < 0.02$) at the low dose (0.5 mg/kg ; $0.645 \text{ } \mu\text{mol/kg}$) and 37.2% ($P < 0.02$) at the higher dose (5.0 mg/kg ; $6.45 \text{ } \mu\text{mol/kg}$). Plasma BSP disappearance rates were similarly affected at both low (0.064 mg/kg ; $0.077 \text{ } \mu\text{mol/kg}$) and higher (10.3 mg/kg ; $12.3 \text{ } \mu\text{mol/kg}$) doses, and again, the disappearance rate of the higher dose was decreased to a greater extent (35.4%; $P < 0.01$) than the low dose (19.3%; $P < 0.01$). With a Lineweaver-Burk plot, it was possible to estimate the corresponding changes in V_{max} and K_m (Table IV). Unlike BR, fasting caused an appreciable decrease in both parameters for

TABLE VI
BSP Loading Studies

BSP dose $\mu\text{mol/kg}$	Studies	Inhibitor	Inhibitor dose $\mu\text{mol/kg}$	k min^{-1}	\pm SD
0.084	5	—	—	0.939	0.010
0.135	3	—	—	0.940	0.027
0.234	3	—	—	0.938	0.080
12.6	6	—	—	0.776	0.081
61.9	3	—	—	0.339	0.030
117.3	3	—	—	0.307	0.025
0.093	3	ICG	14.6	0.361	0.052
0.194	3	ICG	14.6	0.362	0.050
64.5	3	ICG	14.6	0.211	0.025
0.098	4	BR	14.6	0.718	0.050
0.210	3	BR	14.6	0.726	0.009
0.292	3	BR	14.6	0.712	0.006
23.1	3	BR	14.6	0.488	0.014
60.8	4	BR	14.6	0.298	0.021
0.079	5	Glycocholate	50	0.886	0.105
0.052	4	Ethacrinic acid	12.3	0.901	0.093
0.052	4	Ethacrinic acid	30.7	0.693	0.044
0.084	3	Cephalothin	47.8	0.891	0.126
0.103	9	Fasting		0.758	0.040
12.3	9	Fasting		0.501	0.102

Data from BSP loading studies in which the plasma fractional disappearance rate (k) of a tracer dose of $[^3\text{S}]\text{BSP}$ injected with varying amounts of unlabeled BSP was measured with and without accompanying inhibitor and after fasting.

ICG and BSP (ICG: $V_{max} = 2.06 \pm 0.84$, $K_m = 4.26 \pm 2.02$; BSP: $V_{max} = 18.0 \pm 16.5$, $K_m = 23.7 \pm 22$). Since these estimates are calculated from only two sets of data points (D, \bar{V}), they have relatively large uncertainties.

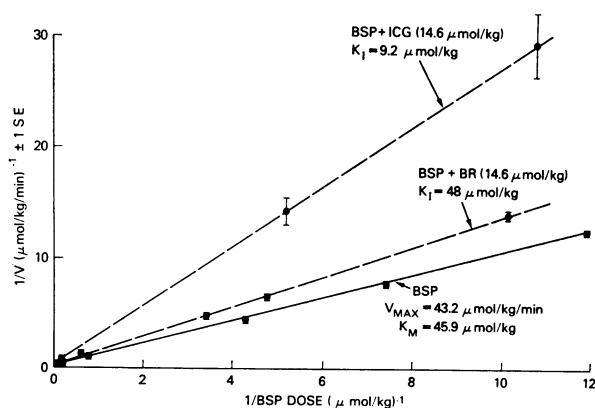


FIGURE 5 Lineweaver-Burk plots of plasma BSP disappearance rates in the absence of inhibitor and in the presence of ICG and BR. Each data point is the mean \pm 1 SE of values obtained from several animals. Note that ICG inhibits plasma BSP disappearance much more effectively than BR.

TABLE VII
Phenobarbital Pretreatment

	Liver wt.		UDPGT activity	BR uptake rate
	% increase	% increase/g liver		%
SD rats	24.4	70.0		24.3
Gunn rats	28.2	0		26.7

The effects of phenobarbital pretreatment (70 mg/kg/day for 1 wk) on liver weight (expressed as percent of body weight), hepatic UDPGT activity, and the plasma disappearance rate of a tracer dose of [³H]BR in both SD and Gunn rats.

Countertransport. Results of the countertransport studies are illustrated in Fig. 6. When an intravenously injected tracer dose of [³H]BR or [³⁵S]BSP was followed 2-7 min later by a large bolus of unlabeled BR, BSP, or ICG, plasma [³H]BR activity stopped declining and began to rise. Similar results were observed when a 0.5 mg/kg dose of ICG was followed by a bolus of unlabeled BR or BSP. Since radiolabeled ICG was not available, it was not possible to inject a tracer dose of ICG followed by a bolus of unlabeled ICG. Thus, both [³H]BR and [³⁵S]BSP showed a net flux from liver to plasma, against the prevailing concentration gradient, after the intravenous injection of a large bolus of unlabeled BR or BSP, respectively. Similarly, [³H]BR, [³⁵S]BSP, and ICG each showed a net flux from liver to plasma when a large dose of a second organic anion, capable of competing with it for hepatic uptake, was injected.

This type of phenomenon has been given the name "countertransport" or "counterflow" (24-26) and cannot be explained by simple diffusion. For [³H]BR, a possible mechanism might be outlined as follows. Briefly, the very large dose of unlabeled BR essentially stops hepatic uptake of [³H]BR by occupying all available "carrier sites." However, it does not acutely inhibit countertransport of [³H]BR from cytoplasm to plasma, since intracellular BR concentration is not immediately affected. In membrane systems simpler than this whole-animal model, countertransport is considered strong evidence for the existence of carrier-mediated transport. Much more detailed discussions of this phenomenon can be found elsewhere (24-26).

DISCUSSION

These studies demonstrate that the hepatic uptake of BR, BSP, and ICG each shows three properties considered strong evidence for the presence of carrier-mediated transport (24-26). These are: (a) saturation with increasing dose; (b) relatively selective, mutually competitive inhibition; and (c) countertransport.

These studies complement work done by previous investigators who have shown (a) that the hepatic uptake of ICG (11, 27, 28), BSP (24, 28, 29), and BR (30) are saturable processes; (b) that ICG inhibits hepatic BSP uptake (29); (c) that BR (11, 29) and BSP (29) inhibit hepatic ICG uptake; and (d) that countertransport may be demonstrated for BSP (31). However, previous studies have not quantitated the parameters of hepatic uptake (V_{max} and K_m), quantitated the relative inhibitory capacities (K_I), or demonstrated countertransport for all three organic anions in the same species.

These data, in addition, provide information about the relationship of hepatic BR uptake to its subsequent conjugation and excretion. For example, normal daily BR production in SD rats is approximately 7 mg/kg/day (32). If the simplifying assumption is made that the entire 7 mg is transported from plasma into the liver, then the normal net transfer rate of BR from plasma into the liver in SD rats is approximately 10 nmol/kg/min. This is less than 1% of 1.44 μ mol/kg/min, the maximal uptake capacity. It would thus seem unlikely that uptake is, under normal circumstances, the rate-limiting step in the overall transport of

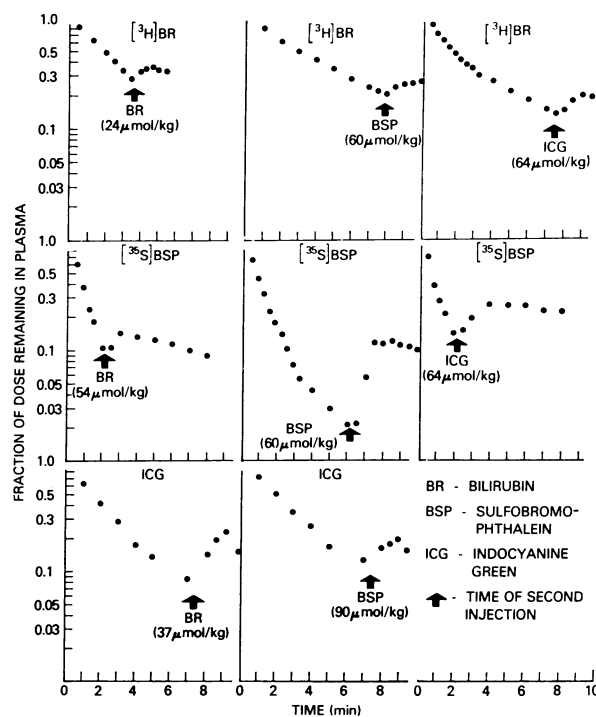


FIGURE 6 [³H]BR, [³⁵S]BSP, and ICG countertransport. A tracer dose of [³H]BR, [³⁵S]BSP, or a 0.5 mg/kg dose of ICG was injected intravenously and followed 2-7 min later (arrow) by a bolus of unlabeled BR, BSP, or ICG. Each of these three organic anions showed reflux from liver to plasma after the second injection.

BR from blood to bile. Results of these studies further suggest that the process of hepatic BR uptake in the rat is unaffected by prolonged fasting (unlike ICG and BSP), and that the increase in uptake rate caused by phenobarbital administration is independent of subsequent glucuronide conjugation.

Several variables complicate the interpretation of values for V_{max} , K_m , and K_i calculated from a whole-animal model such as this. These parameters are very likely influenced by factors such as total hepatic blood flow (which may be rate-limiting for hepatic uptake of some substances at low doses) and the relative affinities of organic anions for albumin, as well as potential membrane carrier sites. In addition, since hepatic sinusoidal blood flows from portal tract to central vein, and BR, BSP, and ICG are all removed relatively rapidly by the liver, periportal hepatocytes are probably exposed to a higher concentration of each of these organic anions than centrilobular cells. The structural arrangement of the hepatic lobule has been given special attention by Goresky (28) in his studies of hepatic BSP uptake.

In spite of these and other factors that dictate caution in interpreting the values calculated for V_{max} , K_m and K_i , results of the inhibitory studies are somewhat surprising. That ICG is a much weaker inhibitor of hepatic BR uptake than BSP does not appear consistent with the observation that ICG inhibits hepatic BSP uptake more effectively than both BR and BSP itself. This observation, as well as the strikingly different maximal transport capacities for these three organic anions, suggest that more than one site may be involved in their uptake.

One other aspect of these results was somewhat unexpected. While it was not possible to demonstrate saturation of hepatic BR uptake in Gunn rats or rats given an infusion of unlabeled BR followed by a tracer dose of [^3H]BR, saturation was readily demonstrated by studies in which rats were given a bolus of BR without prior infusion. This is especially surprising since the calculated initial BR concentration at which half-maximal hepatic uptake occurred (6.2 mg/100 ml) in the bolus injection studies was much less than the highest concentration produced by infusion (53.4 mg/100 ml). A potential explanation for these findings may lie in the differing experimental conditions. Whereas loading studies acutely increase plasma BR concentration without immediately affecting intrahepatic BR concentration, prolonged BR infusion increases both (33). Thus, large doses of BR appear to enter the liver more rapidly when intrahepatic BR concentration is increased by prior BR infusion.

A precedent for this type of finding exists in previous studies of membrane transport in other systems. The observation has been made that glucose is transported

out of human erythrocytes more rapidly in the presence of extracellular glucose than in its absence (34, 35). Other investigators have demonstrated that preloading Ehrlich ascites tumor cells with glycine increases the initial transport rate of labeled glycine into the cell (36). Depending upon the particular experimental model in which it was observed, this type of phenomenon has been called "accelerative exchange diffusion" (26) or "preloading effect" (37) and has been explained with the model of carrier-mediated transport. This model assumes the presence of carriers within the cell membrane. These carriers bind reversibly with substrate at either surface of the membrane to form a complex, and can diffuse (or "move" in some kinetically equivalent fashion) either as free carrier or as complex from one side to the other. In this way, substrate, which by itself diffuses very slowly if at all across the membrane, is transported into or out of the cell.

In these studies, the unidirectional flux of BR into the hepatocyte is measured by the rate of disappearance of labeled BR from the plasma. This unidirectional flux depends upon the rate at which carrier-BR complex diffuses into the cell, as well as the rate of return of carrier molecules to the external surface. If the diffusion rate of free carrier is much slower than that of complex (26), the return of carrier molecules to the external surface would be accelerated by increasing intracellular BR concentration. Thus, infusion studies, which increase intra- and extracellular BR concentration, might be less likely to demonstrate saturation than bolus injection studies.

Other investigators who have emphasized the fact that the "preloading" effect seems to be a property of concentrative transport systems only, have developed an alternative hypothesis (37, 38). This model does not require the assumption that the diffusion rate of free carrier differs from that of complex. Instead, the carrier is postulated to be present in the membrane in two mobile, interconvertible forms that differ in their substrate affinity. Kinetic analysis of this model (37) has shown that it agrees well with published data on the transport of glycine into Ehrlich ascites tumor cells and explains the preloading effect as well as other properties of concentrative membrane transport systems.

Finally, the results of these studies allow speculation about the potential role of cytoplasmic proteins such as "Y" and "Z" (39-49) in organic anion uptake. If cytoplasmic proteins were primarily responsible for organic anion uptake, one might expect that BR infusion would decrease rather than increase uptake rate by saturating these intracellular receptor sites. In addition, previous studies performed by other investigators (47) suggest that ICG readily displaces BR from Y protein, yet results of the current studies suggest that ICG competes

very weakly with BR for hepatic uptake. Also, the generally held model of facilitated transport described above is that of a carrier-mediated process in which movement of the carrier molecules is restricted to within the cell membrane. All of these observations would suggest that cytoplasmic proteins such as Y and Z do not play a primary role in the membrane transport process responsible for the initial uptake of organic anions. Rather, it is probable that they secondarily affect net transport by their function as intracellular "storage" proteins.

REFERENCES

- Berk, P. D., R. B. Howe, J. R. Bloomer, and N. I. Berlin. 1969. Studies of bilirubin kinetics in normal adults. *J. Clin. Invest.* **48**: 2176-2190.
- Dixon, M., and E. C. Webb. 1964. *Enzymes*. Academic Press, Inc., New York. 2nd edition. 54-70, 315-320.
- Howe, R. B., P. D. Berk, J. R. Bloomer, and N. I. Berlin. 1970. Preparation and properties of specifically labeled radiochemically stable ³H-bilirubin. *J. Lab. Clin. Med.* **75**: 499-502.
- Van Roy, F. P., J. A. T. P. Meuwissen, F. De Meuter, and K. P. M. Heirwegh. 1971. Determination of bilirubin in liver homogenates and serum with diazotized *p*-iodoaniline. *Clin. Chim. Acta.* **31**: 109-118.
- Heirwegh, K. P. M., G. P. Van Hees, P. Leroy, F. P. Van Roy, and F. H. Jansen. 1970. Heterogeneity of bile pigment conjugates as revealed by chromatography of their ethyl anthranilate azopigments. *Biochem. J.* **120**: 877-890.
- Weber, A. P., and L. Schalm. 1962. Quantitative separation and determination of bilirubin and conjugated bilirubin in human serum. *Clin. Chim. Acta.* **7**: 805-810.
- Blaschke, T. F., P. D. Berk, B. F. Scharschmidt, J. R. Guyther, J. M. Vergalla, and J. G. Waggoner. 1974. Crigler-Najjar syndrome: an unusual course with development of neurologic damage at age eighteen. *Pediatr. Res.* **8**: 573-590.
- Plotz, P. H., P. D. Berk, B. F. Scharschmidt, J. K. Gordon, and J. Vergalla. 1974. Removing substances from blood by affinity chromatography. I. Removing bilirubin and other albumin-bound substances from plasma and blood with albumin-conjugated agarose beads. *J. Clin. Invest.* **53**: 778-785.
- Black, M., B. H. Billing, and K. P. M. Heirwegh. 1970. Determination of bilirubin UDP-glucuronyl transferase activity in needle-biopsy specimens of human liver. *Clin. Chim. Acta.* **29**: 27-35.
- Gaebler, O. H. 1945. Determination of bromsulphalein in normal, turbid, hemolyzed, or icteric serums. *Am. J. Clin. Pathol.* **15**: 452-455.
- Paumgartner, G., P. Probst, R. Kraines, and C. M. Leevy. 1970. Kinetics of indocyanine green removal from the blood. *Ann. N. Y. Acad. Sci.* **170**: 134-147.
- Scharschmidt, B. F., P. D. Berk, and J. G. Waggoner. 1973. Bilirubin (BR) kinetics in the normal rat. *Clin. Res.* **21**: 523. (Abstr.)
- Berman, M., and M. F. Weiss. 1967. Users' manual for SAAM. United States Public Health Service Publication No. 1703. United States Department of Health, Education and Welfare, Washington, D. C., United States Government Printing Office.
- Lewis, A. E., R. D. Goodman, and E. A. Schuck. 1952. Organ blood volume measurements in normal rats. *J. Lab. Clin. Med.* **39**: 704-710.
- Berman, M. 1963. The formulation and testing of models. *Ann. N. Y. Acad. Sci.* **108**: 182-194.
- Berman, M., and R. Schoenfeld. 1956. Invariants in experimental data on linear kinetics and the formulation of models. *J. Appl. Physiol.* **27**: 1361-1370.
- Quarfordt, S. H., H. L. Hilderman, D. Valle, and E. Waddell. 1971. Compartmental analysis of sulfobromophthalein transport in normal patients and patients with hepatic dysfunction. *Gastroenterology.* **60**: 246-255.
- Berk, P. D., T. F. Blaschke, and J. G. Waggoner. 1972. Defective bromosulfophthalein clearance in patients with constitutional hepatic dysfunction (Gilbert's syndrome). *Gastroenterology.* **63**: 472-481.
- Mikulecky, M. 1973. The compartmental analysis of indocyanine green plasma clearance in normal human subjects with the aid of a digital computer. *Scr. Med. (Brno.)* **46**: 469-476.
- Blaschke, T. F., R. J. Elin, P. D. Berk, C. S. Song, and S. M. Wolff. 1973. Effect of induced fever on sulfobromophthalein kinetics in man. *Ann. Intern. Med.* **78**: 221-226.
- Cohn, C., R. Levine, and D. Streicher. 1947. The rate of removal of intravenously injected bromsulphalein by the liver and extrahepatic tissues of the dog. *Am. J. Physiol.* **150**: 299-303.
- Cohn, C., R. Levine, and M. Kolinsky. 1948. Hepatic and peripheral removal rates, in the dog, for intravenously injected bromsulphalein. *Am. J. Physiol.* **155**: 286-289.
- Leevy, C. M., J. Bender, M. Silverberg, and J. Naylor. 1963. Physiology of dye extraction by the liver: comparative studies of sulfobromophthalein and indocyanine green. *Ann. N. Y. Acad. Sci.* **111**: 161-175.
- Goresky, C. A. 1965. The hepatic uptake and excretion of sulfobromophthalein and bilirubin. *Can. Med. Assoc. J.* **92**: 851-857.
- Kotyck, A., and K. Janáček. 1970. *Cell membrane Transport Principles and Techniques*. Plenum Publishing Corporation, New York. 55-89.
- Stein, W. D. 1967. *The movement of molecules across cell membranes*. Academic Press, Inc., New York. 126-176.
- Leevy, C. M., F. Smith, J. Longueville, G. Paumgartner, and M. M. Howard. 1967. Indocyanine green clearance as a test for hepatic function. Evaluation by dichromatic ear densitometry. *JAMA (J. Am. Med. Assoc.)* **200**: 236-240.
- Goresky, C. A. 1964. Initial distribution and rate of uptake of sulfobromophthalein in the liver. *Am. J. Physiol.* **207**: 13-26.
- Hunton, D. B., J. L. Bollman, and H. N. Hoffman II. 1961. The plasma removal of indocyanine green and sulfobromophthalein: effect of dosage and blocking agents. *J. Clin. Invest.* **40**: 1648-1655.
- Goresky, C. A. 1975. The hepatic uptake process: its implications for bilirubin transport. In *Jaundice*. C. A. Goresky and M. M. Fisher, editors. Proceedings of the Second International Symposium of the Canadian Hepatic Foundation. Plenum Press, New York.
- Brauer, R. W. 1961. Paper presented to the American Association for the Study of Liver Disease. Chicago, Illinois. Quoted in ref. 24.
- Gisselbrecht, C., and P. D. Berk. 1974. Failure of

- phenobarbital to increase bilirubin production in the rat. *Biochem. Pharmacol.* **23**: 2895-2905.
33. Billing, B. H., Q. Maggiore, and M. A. Carter. 1963. Hepatic transport of bilirubin. *Ann. N. Y. Acad. Sci.* **111**: 319-325.
 34. Levine, M., D. L. Oxender, and W. D. Stein. 1965. The substrate-facilitated transport of the glucose carrier across the human erythrocyte membrane. *Biochim. Biophys. Acta.* **109**: 151-163.
 35. Mawe, R. C., and H. G. Hempling. 1965. The exchange of C¹⁴ glucose across the membrane of the human erythrocyte. *J. Cell. Comp. Physiol.* **66**: 95-103.
 36. Heinz, E. 1954. Kinetic studies on the "influx" of glycine-1-C¹⁴ into the Ehrlich mouse ascites carcinoma cell. *J. Biol. Chem.* **211**: 781-790.
 37. Silverman, M., and C. A. Goresky. 1965. A unified kinetic hypothesis of carrier mediated transport: its applications. *Biophys. J.* **5**: 487-509.
 38. Rosenberg, T., and W. Wilbrandt. 1963. Carrier transport uphill. I. General. *J. Theor. Biol.* **5**: 288-305.
 39. Levi, A. J., Z. Gatmaitan, and I. M. Arias. 1969. Two hepatic cytoplasmic protein fractions, Y and Z, and their possible role in hepatic uptake of bilirubin, sulfobromophthalein, and other anions. *J. Clin. Invest.* **48**: 2156-2167.
 40. Reyes, H., A. J. Levi, Z. Gatmaitan, and I. M. Arias. 1969. Organic anion-binding protein in rat liver: drug induction and its physiologic consequence. *Proc. Natl. Acad. Sci. U. S. A.* **64**: 168-170.
 41. Levi, A. J., Z. Gatmaitan, and I. M. Arias. 1969. Deficiency of hepatic organic anion-binding protein as a possible cause of non-haemolytic unconjugated hyperbilirubinaemia in the newborn. *Lancet.* **2**: 139-140.
 42. Levi, A. J., Z. Gatmaitan, and I. M. Arias. 1970. Deficiency of hepatic organic anion-binding protein, impaired organic anion uptake by liver and "physiologic" jaundice in newborn monkeys. *N. Engl. J. Med.* **283**: 1136-1139.
 43. Grodsky, G. M., H. J. Kolb, R. E. Fanska, and C. Nemecek. 1970. Effect of age of rat on development of hepatic carriers for bilirubin: a possible explanation for physiologic jaundice and hyperbilirubinemia in the newborn. *Metab. Clin. Exp.* **19**: 246-252.
 44. Levine, R. I., H. Reyes, A. J. Levi, Z. Gatmaitan, and I. M. Arias. 1971. Phylogenetic study of organic anion transfer from plasma into the liver. *Nat. New Biol.* **231**: 277-279.
 45. Litwack, G., B. Ketterer, and I. M. Arias. 1971. Ligandin: a hepatic protein which binds steroids, bilirubin, carcinogens and a number of exogenous organic anions. *Nature (Lond.)*. **234**: 466-467.
 46. Reyes, H., A. J. Levi, Z. Gatmaitan, and I. M. Arias. 1971. Studies of Y and Z, two hepatic cytoplasmic organic anion-binding proteins: effect of drugs, chemicals, hormones and cholestasis. *J. Clin. Invest.* **50**: 2242-2252.
 47. Kamisaka, K., I. Listowsky, and I. M. Arias. 1973. Circular dichroism studies of Y protein (ligandin), a major organic anion-binding protein in liver, kidney, and small intestine. *Ann. N. Y. Acad. Sci.* **226**: 148-161.
 48. Fleischer, G., R. Kirsch, K. Kamisaka, I. Listowsky, Z. Gatmaitan, W. Habig, M. Pabst, W. B. Jakoby, and I. M. Arias. 1974. Identity of ligandin (Y protein) and glutathione transferase B: its role in ethacrinic acid metabolism and organic anion transport in kidney and liver. *Gastroenterology.* **67**: A15/792 (Abstr.).
 49. Habig, W. H., M. J. Pabst, G. Fleischer, Z. Gatmaitan, I. M. Arias, and W. B. Jakoby. 1974. The identity of glutathione S-transferase B with ligandin, a major binding protein of liver. *Proc. Natl. Acad. Sci. U. S. A.* **71**: 3879-3882.